We are IntechOpen,
the world's leading publisher of
Open Access books
Built by scientists, for scientists

4,800
Open access books available

122,000
International authors and editors

135M
Downloads

Our authors are among the

154
Countries delivered to

TOP 1%
most cited scientists

12.2%
Contributors from top 500 universities

CLARIVATE ANALYTICS
BOOK CITATION INDEX
INDEXED

WEB OF SCIENCE™

Selection of our books indexed in the Book Citation Index
in Web of Science™ Core Collection (BKCI)

Interested in publishing with us?
Contact book.department@intechopen.com

Numbers displayed above are based on latest data collected.
For more information visit www.intechopen.com

Structural Aspects of Anatase to Rutile Phase Transition in Titanium Dioxide Powders Elucidated by the Rietveld Method

Alberto Adriano Cavalheiro,

Lincoln Carlos Silva de Oliveira and

Silvanice Aparecida Lopes dos Santos

Additional information is available at the end of the chapter

Abstract

Titanium dioxide has attracted much attention since a long time ago due to its versatility as advanced material. However, its performance as semiconductor devices is very much dependent on the predominant crystalline phase and defect concentrations, which can be adjusted through the synthesis methods, thermal treatments and doping processes. In this work, an accurate structural characterization of titanium dioxide was used by X-ray diffractometry supported by rietveld refinement and thermal analysis. The insertion of 5 mol% of zirconium silicate was able to stabilize anatase up to 900°C, permitting the oxygen vacancies to be significantly eliminated. It was demonstrated also that the changes in the isotropic thermal parameters for oxygen are related to reconstructive transformation necessary to promote the anatase-to-rutile phase transition. Independently of doping process, the crystallization process of anatase phase as a function of temperature increasing occurs exclusively due the reduction of lattice microstrain up to 600°C. However, above 650°C, that crystallization process becomes dependent of the increasing in crystallite size. The anatase crystallite growth event was only possible when the titanium dioxide was doped with zirconium silicate. Otherwise, the rutile phase amount starts to rise continually. Thus, there are optimistic expectations for that new composition to be a new semiconductor matrix for additional doping processes.

Keywords: sol-gel method, isovalent doping, phase transition, XRD, rietveld refinement

1. Introduction

The titanium dioxide TiO_2 is a semiconductor ceramic material widely applied for polluted water remediation and self-cleaning surfaces. The main basis of titanium dioxide powder and thin film performance is the electron excitation from valance band to conducting one, which can be carried out by lighting the material surface with radiation energy greater than its band gap. Thus, the larger the number of electron-hole pairs, the greater the rate of degradation of organic compounds by oxy-reduction [1–5].

There are some mechanism details to be considered after the initiation of lighting process and the final mineralization of organic compounds, which can be changed as a function of the organic molecule type and its semi-decomposed by-products, organics concentration and pH of solution, distance between the radiation source and the semiconductor material, radiation intensity and losses in the optical path, as well as some characteristics of the powder or thin film morphologies. But, the characteristic of the titanium dioxide semiconductor is the most important factor to be considered, including the morphology, composition and crystalline structure [6–9].

First of all, the importance of solid morphology is an intuitive aspect due to the basis of heterogeneous catalysis, and the several papers on the literature relating to the synthesis of titanium dioxide nanoparticles provide a good idea of the importance of a large specific area for powders. Innovative semiconductor arrangements like p-n junction, titanium dioxide glass-ceramic, ion-sodium battery based on anatase titanium dioxide ceramic matrix are also investigated in order to provide new applications concerning novel structures and morphologies degrees, making the titanium dioxide much more investigated [10–12].

In sequence, at first sight, the composition aspect seems not be applicable because high purity titanium dioxide should have stoichiometry defined as TiO_2. However, the fact is titanium dioxide is an intrinsic N-type semiconductor due to oxygen vacancies generated during the heat treatment, mainly for samples with high amount of anatase phase. Nevertheless, the non-doped n-type anatase titanium dioxide powder or thin films are usually applied as photocatalyst materials in advanced oxidation process for organic compounds. The justification is based on the yield of long-lived extrinsic photoholes, which is able to promote the water oxidation [13, 14].

The non-stoichiometry characteristic of titanium dioxide is very similar to the zinc oxide, so that many investigations consider the addition of extrinsic dopants in order to change semiconductor predominant behaviour. But, when the concentration of cation dopants becomes higher or when anion dopants are inserted in oxygen site, the crystalline structure starts to play an important role. In general, metallic cations with different oxidation states than tetravalent titanium are investigated and the energy bandgap and other photonic aspects are availed [15–17]. But, tetravalent titanium vacancies can be also formed through alternative procedures in order to generate some interesting properties, like high p-type conductivity and better photocatalytic performance [18].

Several works repot related the insertion of heterovalent metallic cations in titanium dioxide lead to the decreasing in the temperature of anatase-to-rutile phase transition and also to more amounts of rutile phase if the powder samples are heat treated up to 600°C [19–22]. Most of the

doping approaches aim to shift the absorption edge to lower frequencies than ultraviolet range in order to utilize the titanium dioxide in solar photocatalysis. The nitrogen insertion by replacing lattice oxygen in anatase phase of titanium dioxide has also this central objective. However, there are strong suspicions that the desired surface electronic enhancement was followed by a considerable lattice surface distortion [23, 24].

The most of the doped titanium dioxide structures present different effects for anatase and rutile polymorphism due to the not well-controlled sample preparation as well as overlapping of several different effects. The oxygen vacancies seem to occur in association with most dopant insertion, and their concentrations are very sensitive to heat treatments. In addition to the lattice distortions and the changes in cation gap states caused by doping process, the oxygen vacancies also act as hole-trapping sites [25–27].

Even for that high-ordered single-crystal rutile sample, the trivalent titanium acting as trap site in (110) surface was found [28]. Any of those events seems to be significantly responsible for the enhancing or damaging of the titanium dioxide photocatalyst performance. Thus, well-characterized structural model systems are required to understand other changes in the material bulk or surface [29].

The exclusive structural aspects deserve special attention in order to understand a little more about the interfacial charge transfer in complex surface structure of the titanium dioxide photocatalyst, because the free energy on the single crystal surface is affected by its crystallographic orientation [30]. Different crystallographic planes were investigated separately in single crystal samples, and an interesting hypothesis was proposed concerning the surface atoms alignment. A reasonable experiment set including the etching of high aligned (001) facet proved that the more aligned the oxygen and titanium atoms on the surface, the greater are the chances of recombination of the electron-hole pairs [27].

The mechanisms of chemical reaction as a function of crystalline phase are also investigated. The single crystalline rutile (110) and anatase (101) samples submitted to the oxygen and water adsorptions at low temperatures, during the reheating up to room temperature, can be very useful to understand several aspects of photocatalysis mechanisms. Both rutile (110) and anatase (101) surfaces experience the reaction between oxygen and water molecules in order to form terminal hydroxyl groups on the phase surfaces. While the hydroxyl groups formed on the rutile (110) surface are highly bridged, on the anatase (101) surface the hydroxyl groups remain isolated and stable even after annealing above 130°C. The water molecules desorbs readily at room temperature from anatase (101) surfaces, whereas the oxygen ones remain undissociated and adsorbed in the vicinity of extrinsic P-type defects, and those differences have important consequences for photocatalysis application [31].

It is well understood that the anatase-to-rutile phase transition in polycrystalline titanium dioxide powder samples is strongly dependent on the anatase phase characteristics, mainly the impurity amount and the extrinsic dopant type. But, some structural surface aspects for non-doped and high purity powder samples are also indicative signals, such as the nucleation of the rutile phase by anatase (112) surface. A different intermediate metastable phase dissimilar to the prior anatase or the final rutile phases was observed, which showed to be sensitive to the compressive strain and the phase anisotropy [32, 33].

The photonic behaviour is strongly influenced by predominant phase characteristics, but some results attributed to the partial anatase-to-rutile phase transition through the controlled heat treatment leading to an enhancement in the photocatalytic performance. However, this hypothesis is controversial, because there are serious evidences that the anatase-to-rutile phase transition can start only the previous ordering in anatase phase. Thus, the relationship between well-crystallized anatase structure and photocatalytic activity can aid to understand some aspects not yet clarified about this material [34, 35].

The irreversible anatase-to-rutile phase transition occurring in temperatures above 600°C is a well-known fact for any experienced researcher working with titanium dioxide samples. It is also easy to verify that increasing the rutile phase amount is proportional to the temperature of heat treatment beyond 600°C. The anatase phase in titanium dioxide powder samples can be obtained even at room temperatures if no high amounts of organics are present in precursor materials, such as that provided by conventional sol-gel method. No structural differences seem to occur between the fresh hydrolysed samples and the heat treated one until 150°C, because the anatase phase nuclei is a water-driven process in order to form oxy-hydroxide titanium, which is relatively stable up to 150°C [36–38].

The continuous increase in temperature of heat treatment triggers several sequential decomposition stages in fresh hydrolysed gels, concerning the elimination of several residual compounds, such as the adsorbed water, hydroxyl groups and organic by-products. Unless the organic by-product types are able to form carbonaceous solid compounds, above the 250°C, the anatase phase is already an impurity-free material. Nevertheless, the desidroxylation stage is followed by the formation of cross-linked nuclei, which creates high amount of structural defects, in special, the oxygen vacancies. Those defects only can be eliminated overcoming the energy barrier of titanium-oxygen bonds, which leads to the structural destroy-rebuilding processes. This mechanism is the basis of the reconstructive transformation observed in the anatase-to-rutile phase transition [24, 32] and that is why the effective anatase phase crystallization only occurs when the rutile phase starts to form.

It was demonstrated earlier that the oxygen vacancies in titanium dioxide material configure an N-type semiconductor, which seems to be a not good photocatalyst due to high electron-hole combination occurring in oxygen vacancies. In addition, the formation of hydroxyl radical in aqueous media is also dependent on positive holes. Consequently, several dopants with lower oxidation states than titanium (IV) are investigated in order to make that material a P-type semiconductor [23].

In parallel, the synthesis method also plays an important role on the anatase crystallization and the sol-gel method is one of the most used to synthesize titanium dioxide powder and thin film samples. That chemical route is able to synthesize well-crystallized titanium dioxide samples with anatase single phase at very low temperature because the titanium dioxide formation is a water-driven process that occurs even at room temperature and leads invariably to anatase single phase. It is possible to use only volatile coadjutant reagents, such as the metallic alkoxide precursors and acetic acid complexing agent, so that very little amount of organic wastes gets retained when the fresh gels are dried at 100°C or almost nothing if dried above 150°C. There is no chance for the existence of organic solid residues, even if metallic

nitrates are used as dopant precursor reagents, which makes the sol-gel method the preferential choice in order to obtain nanoparticles of titanium dioxide in anatase single phase with relative success [39].

In addition, the amounts of alcohol solvent and water as hydrolyzing agent are also important on the particle growth stage, because the cross-linked bonds are affected directly by those coadjutant reagents during the first stages of titanium oxy-hydroxide nuclei formation. It is almost a consensus that the mean particle diameter reduces as a function of water content in the jellifying process [40], due to the more separation of nuclei from each other. Nevertheless, that means a more amount of terminal hydroxyl groups in anatase phase particle surface and, consequently, a more amount of cross-linked bonds emerging during the drying stage.

The anatase thermal stability depends on the defect concentration, including the oxygen vacancies. The oxygen vacancies concentration can be dependent on the amount of the cross-linked bonds among the nanoparticles so that the titanium dioxide nanoparticles can present a significant increase in oxygen vacancies when compared to the coarse particles. Thus, the literature shows that the thermal treatment to crystallize the titanium dioxide nanoparticles is preferentially carried out in temperatures below 500°C, which is still far from the energetic barrier for anatase-to-rutile phase transition [41]. Less often, the nanoparticles can be carefully thermal treated under step-by-step process by increasing the temperature from 250 to 600°C, at most, if it is desirable to obtain anatase single phase [42], which is probably due to the lower stability for anatase phase in nanoparticle form [43, 44].

On the other hand, homovalent cation doping seems to reduce also the oxygen vacancies, which can also be associated with cross-linked metal-oxygen bonds in anatase phase. The insertion of zirconium at 10 mol% in titanium dioxide powder samples avoids the full anatase-to-rutile phase transition at higher temperatures than 600°C, leading to the calcined material to present high amounts of anatase phase when calcined up to 750°C. By increasing the zirconium content and calcining the material at same temperature, much more amounts of anatase phase are observed in powder samples. However, an orthorhombic zirconium titanate secondary phase starts to crystallize in addition to the remaining anatase phase when the zirconium content is higher than 10 mol% [45].

By comparing the ionic radii for Ti (IV) and Zr (IV) hexacoordinate cations, it is possible to infer that the zirconium cation is bigger (72 pm) than titanium one (61 pm) [46]. As consequence, if the zirconium substitution in titanium site was successful, then a proportional anatase lattice expansion must be observed as a function of zirconium content until at certain concentration limit, at least [28, 45].

Another homovalent cation dopant investigated for anatase phase stabilization is the tetravalent silicon [47]. Thermal analysis from fresh gel has shown that the presence of silicon dopant can delay the anatase crystallization, which can be visualized by an exothermic peak, towards higher temperatures than undoped titanium dioxide. The cell volume for several calcined samples decreases continually as a function of silicon content, besides the crystallinity loss, as visualized by the X-ray diffraction patterns followed by rietveld refinement. The calcined samples in wide temperature range show an increase in temperature of anatase-to-rutile phase

transition, but until a certain dopant concentration limit, signalled as 5 mol%. Different from zirconium dopant, the silicon one does not seem to generate secondary phases, but only to increase the atomic disordering in anatase phase [48]. Those results imply that the silicon dioxide can have infinite solubility in anatase titanium dioxide phase.

Some researchers have believed that the silicon cation is so smaller that its perfect accommodation in interstitial of titanium and oxygen sites of low dense anatase phase is possible. Thus, the explanation for anatase stabilization is justified, because the high dense rutile phase does not have enough interstitial space to accommodate hexacoordinate tetravalent silicon cations, avoiding the phase transition. That consideration is reasonable but is not true, because the ionic radii for hexacoordinate silicon (VI) is 40 pm [46], which means the titanium and silicon cations should experience some repulsion with each other to lead a lattice expansion in anatase phase, which is not observed in the literature.

Furthermore, an important ab-initio study taking into account the alternative silicon dopant positions in anatase and rutile phases buries the idea of interstitial silicon in titanium dioxide sample once and for all. The calculated results suggest that the interstitial tetravalent silicon cation is energetically favourable neither for anatase phase nor for rutile one. Also, the calculated results are in concordance with lattice parameter contraction; thus, it is not a good idea to continue with the consideration of interstitial tetravalent silicon cations in titanium dioxide anatase phase as the cause for anatase stabilization. At least while the X-ray diffraction data are showing the consistent anatase lattice contraction for silicon-doped titanium-doped powder samples [29].

The stabilization of anatase phase caused by homovalent dopants seems to be related to the increase in cross-linked metal-oxygen bond energies still in anatase phase. In addition, the reported enhancement in photocatalytic performance for homovalent doping cannot be related exclusively to the decrease in oxygen vacancies [28]. The effect in crystal surface can play an important role in order to reduce the recombination of electron-hole pair, and the anatase phase surface presenting oxygen and cations outer of the plane seems to be crucial to avoid that auto-neutralizing phenomenon [10, 31].

The first attempt to use simultaneously silicon and zirconium dopants was published in 2006 [49] but did not contribute to the correct understanding of the anatase phase stabilization in titanium dioxide samples. First, because the anatase phase stabilization occurring as a function temperature increasing or even significant changes in anatase-to-rutile phase transition were not demonstrated, according the X-ray diffraction patterns available on that work. Except at 700°C, all of the samples presented rutile phase and the authors chose to explain the results by considering no dopant substitutions, but the effect of anatase interparticle secondary phases.

In addition, considerable confusion can occur if the dopant concentrations were referred as weight percent, due to the enormous difference in atomic weight among the metal constituents, and is not a good choice in order to permit the correct understanding of the progressive doping effects. The results provided by simultaneous and equal weight doping elements for silicon and zirconium at 5 wt% [51] correspond to 8.4 mol% for silicon and 2.6 mol% for

zirconium, which means a Si/Zr molar ratio more than 3. Even so, no considerable differences were observed comparing the isolated zirconium or silicon doping under the point of view of anatase phase stabilization [47, 48, 50–52].

Other consideration about the mechanism of the anatase-to-rutile phase transition is no longer valid, specially, the affirmation that the anatase phase starts to convert into rutile one at lower temperatures through particle agglomeration in a kinetically controlled reaction. It was demonstrated already that there is a thermodynamic stability for anatase phase at standard conditions of temperature and pressure [29], which is determined probably by titanium-oxygen bond energies [24]. The kinetic component starts to play an important role only after overcoming the energetic barrier at very high temperatures, like above 900°C [28].

Only in 2016, another publication reporting the silicon-zirconium-doped titanium dioxide sample was found [53]. There are several doped titanium dioxide nanoparticles calcined at 500°C only, but unexpectedly, the authors discuss about the anatase-to-rutile phase transition as a function of dopant type for anatase single phase samples. In addition, a sample containing only silicon and zirconium dopants was also not prepared so that it was not possible to evaluate the effects of the simultaneous silicon and zirconium doping on titanium dioxide. Despite that the authors affirm that the sample simultaneously doped with copper, silicon and zirconium cations at 15 mol% in total concentration and equal parts showed a great improvement in photocatalytic performance for the degradation of methyl orange.

No other articles about the simultaneous silicon- and zirconium-doped titanium dioxide sample were found in the literature. That way, the present work aims to provide an accurate investigation about exclusive and simultaneous silicon and zirconium doping in titanium dioxide powder samples obtained through the sol-gel method in order to demonstrate the structural basis of anatase phase stabilization. It is very important to keep in mind that equal parts of tetravalent silicon and zirconium cations represent the average ionic radii close to the tetravalent titanium cation, considering all of those in hexacoordinate sites. It is also important to know that zircon silicate $ZrSiO_4$ possesses also anatase phase, which can be thermally stable until very high temperatures [46, 54].

2. Materials and methods

In order to provide a consistent discussion about the influence of the zirconium-silicon simultaneous doping, the non-modified titanium dioxide samples were prepared in the same experimental conditions used to obtaining the doped samples. It was used the true sol-gel method involving only analytical grade reagents for the preparation of the powder samples. First, titanium (IV) isopropoxide 97% (Sigma-Aldrich) was added drop wise in glacial acetic acid 99.7% (F. Maia) under stirring. The molar ratio between the acetic acid and total metallic cations was adjusted to 4 for both samples. Due to the exothermic reaction, the homogenous mixture was cooled to room temperature by maintaining stirring for 30 min before the next step. For silicon-zirconium (Si-Zr)-doped titanium dioxide sample, tetraethyl orthosilicate 98% (Sigma-Aldrich) and zirconium (IV) propoxide 70% (Sigma-Aldrich) are added in order to obtain 5 mol

% of Si-Zr doping. Then, for both samples, the isopropyl alcohol R.G. (Qhemis) was added in order to adjust the metal concentration to 0.1 molar.

After a homogenization stage through the stirring for 30 min, acidified water was added in order to promote the acid hydrolysis. For that proposes, nitric acid solution with pH 3.5 was previously prepared in order to represent a molar ratio between water and metallic cations close to 5. Thus, both composition sols were stirred for 1 hour, capped and allowed to stand at ambient conditions for 24 hours in order to complete the jellification. Both xerogels showed transparent characteristics before the drying process carried out in drying oven at 100°C overnight and ground process in porcelain mortar. Finally, both dry gel samples were divided into several aliquots in order to perform the calcination step in wide range of temperature for 2 hours in a muffle type oven under static atmosphere. The expected compositions are TiO_2 and $Si_{0.25}Zr_{0.25}Ti_{0.95}O_2$, for pure and Si-Zr-doped titanium dioxide-calcined powder samples, respectively.

Both dry gel compositions were characterized by simultaneous thermogravimetric and differential thermal analysis (TG/DTA) in order to verify basic differences between non-doped and Silicon-zirconium-doped gel sample along the temperature of thermal treatment. For that characterization, aliquots close to 100 mg were placed in alumina crucibles and compared with the same amount of alpha-alumina powder as standard material. Sample and reference material crucibles were submitted to heating rate of 10°C min^{-1} from room temperature up to 900°C under synthetic air flux of 10 mL min^{-1} by using a Netszch—Thermische Analyse equipped with TASC 414/2 controller and Pt 10 thermocouples.

The dry gel at 100°C and all of the calcined powder samples in a wide temperature set were characterized by X-ray diffractometry by using D5005 Siemens equipment operating with K-alpha nickel-filtered Cu radiation from 20 to 80° (2-theta) in step scan mode in order to collect the diffraction signal in intervals of 0.02° (2-theta) during 1 s. The obtained diffraction patterns were phase identified using the JCPDS data bank [54], and the anatase and rutile structural models were taken from ICSD data bank [55]. The raw files were refined starting from the chosen anatase and rutile structural models by rietveld method [56] performed with the last upgraded DBWS software [57, 58] in order to include the size-strain calculation.

3. Results and discussion

Figure 1(a) shows the TG/DTG/DTA curves for both dry gel samples, where it is possible to observe higher weight losses for Si-Zr-doped titanium dioxide dry gel in all of the weight loss stages from room temperature up to 460°C. The first weight loss is an endothermic event associated to the volatilisation processes of residual alcohols and acetic acid, including probable ester and nitro compounds, which possess boiling temperatures up to 100°C. In addition to the slight narrow endothermic peak observed for Si-Zr doped titanium dioxide dry gel, the volatile compounds present in that sample were 1.7%, against 1. 3% for pure one, considering the final temperature at 180°C for both curves, according to the DTA peaks.
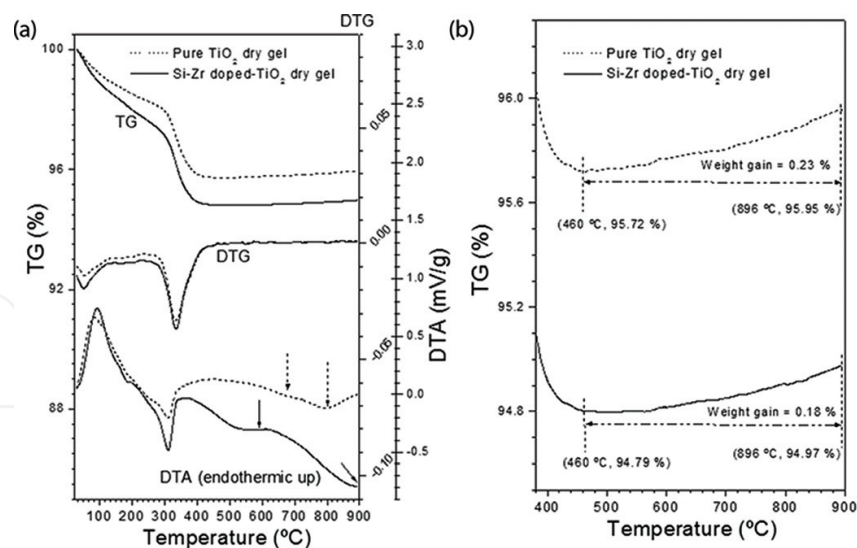
Figure 1. Thermogravimetric and differential thermal analysis for pure and silicon-zircon-doped titanium dioxide dry gel samples: (a) entire TG/DTG/DTA curves and (b) amplification of TG curves between 390 and 900°C.

Residual organic compounds and free-water are desorbed from porous matrixes between 180 and 250°C, markedly a kinetic event, as can be verified by the absence of DTG or DTA peaks in that region. That desorption event represented a weight loss of 0.7% for Si-Zr-doped titanium dioxide dry gel, against 0.4% for the same event in pure titanium dioxide sample. Thus, the total weight losses observed for Si-Zr-doped and pure titanium dioxide dry gels from 30 to 250°C increase for 2.4 and 1.7%, respectively.

The first exothermic event for both samples occurs between 250 and 460°C, which was associated to the cross-link bonding among the hydroxyl groups in nuclei surface through the dehydroxylation process. The water losses associated to that event were close to 2.8% for Si-Zr-doped titanium dioxide sample and 2.6% for pure one. It is also possible to notice that the exothermic peaks (DTA) precede the water weight loss (DTG) in almost 20°C, which prove that the water loss is slower than the dehydroxylation process.

Supposedly, this result is coherent with expected reduction of empty volume among the nuclei due to the pore constriction associated to the cross-link bonding, which harms the water desorption. It is also possible to notice that the exothermic peak for Si-Zr-doped titanium dioxide sample is considerably more intense than that observed for the pure one. Then, already during the dehydroxylation process, an important energetic difference is observed for zircon silicate titanium dioxide samples when compared to the pure one, which can justify possible changes in photocatalysis performances due to the important role the hydroxyl groups in anatase surface have in charge transference and electron-hole recombining processes.

Finally, the anatase crystallization process is observed after the last weight loss and the Si-Zr-doped titanium dioxide samples present two evidenced exothermic events. According to correlated work [59], the presence of silicon dioxide in titanium dioxide seems to favour the crystallization process as a facilitator of the oxygen vacancy elimination. In fact, it is possible to

visualize that the Si-Zr-doped titanium-doped sample has both events more exothermically energetic than the pure one. But, other considerable differences are also observed concerning the temperature of maximum energy. The Si-Zr-doped titanium sample possesses the first crystallization stage starting below 400°C, already during the cross-link bonding, and ends at 550°C. For the pure titanium dioxide sample, there is only a shoulder at 650°C in DTA curve, which is very difficult to view without the graphic software help.

Taking into account that the shoulder in pure titanium dioxide sample occurs above the typical anatase-to-rutile phase transition, it is possible to infer that some amounts of rutile phase probably is already present at that 650°C. Thus, the third exothermic event for pure-doped titanium-doped sample is centred at 800°C, probably associated to the complete formation of rutile phase. On the other hand, the Si-Zr-doped titanium dioxide sample presents the third exothermic event probably above 900°C (not observed due the analysis ending). Nevertheless, there is no evidence that the rutile phase is already present above 900°C, because the zircon silicate has an increasingly stable anatase structure with increasing calcination time and temperature. Thus, 5 mol% of Si-Zr may be sufficient to prevent the rutile phase transition in titanium dioxide samples calcined until 900°C, at least.

Figure 1(b) shows the amplification of TG curves between 390 and 896°C in order to show the weight gain for both samples starting to occur immediately after the final weight loss. Then, it is acceptable that the hypothesis based on oxygen vacancies elimination starts after the ending of cross-link bonding. Both titanium dioxide samples present significant weight gain due to the oxygen incorporation. However, the pure titanium dioxide sample presents higher 0.5% more oxygen incorporation than the Si-Zr-doped one. In addition, the weight gain for Si-Zr-doped sample only becomes remarkable after 550°C.

One important relation between both the samples related to the anatase phase stabilization can be established by considering that the oxygen incorporation is not finished at 900°C due to the kinetic component. Thus, more weight gain can continue to occur until both samples reach a similar weight gain values. If it is true, then the velocity constant for oxygen incorporation in the Si-Zr-doped sample is lower because the same weight gain is reached for pure sample at 811°C, which represents 85°C lower than the Si-Zr-doped sample. An accurate investigation of that dependence would be very interesting to clarify the energetic changes provided by simultaneous silicon-zirconium doping process.

In **Figure 2**, X-ray diffraction patterns showing the phase evolution starting from 100°C for 24 hours to 900°C for 2 hours are shown. The pure titanium dioxide sample presents anatase single phase up to 600°C, which means the rutile phase starts to form at 650°C, according to DTA analysis evidence. On one hand, a continuous increase in temperature of calcination leads to much more rutile phase in the samples until the formation of rutile single phase in pure titanium dioxide powder samples above the 800°C (**Figure 2(a)**). On the other hand, the Si-Zr-doped titanium dioxide samples present no evidence of rutile phase even at 900°C (**Figure 2(b)**).

The angle degrees and the relative intensities for anatase phase peaks in all of the calcination temperatures fit with those available on JCPDS card number 21-1272, whereas the rutile phase
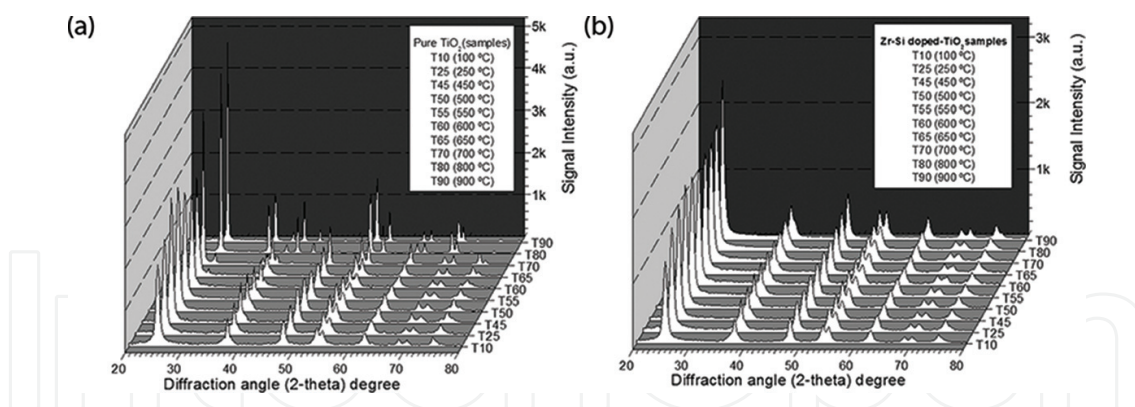
Figure 2. X-ray diffraction patterns showing the phase evolution for starting from 100°C for 24 hours up to 900°C for 2 hours: (a) pure and (b) Si-Zr titanium dioxide samples.

was perfectly identified with the angle degrees and the relative intensities available on JCPDS card number 21-1276. Nevertheless, it is easy to observe a considerable peak enlargement for Si-Zr-doped samples for all temperatures, if compared to the pure ones. However, neither the angle degrees nor the relative intensities are changed for the anatase peaks in Si-Zr-doped titanium dioxide samples along the temperature of calcination.

In order to understand the structural effects beyond the visual observation of the X-ray diffraction patterns, a structural refinement was carried out for all of the samples. That procedure starts choosing the structural models for anatase and rutile phase available on the ICSD data bank. The best adequacy was obtained by setting the lattice parameters and atomic positions according to card numbers 82084 and 53997, for anatase and rutile phase, respectively. After more than 3000 cycles, the refinement factors reach the minimum permitted for statistically expected values provided by method. More information about that methodology is available on the specific literature [56–58, 60].

The lattice parameters of each phase are shown in **Figure 3**. It is possible to observe a consistent variation for all of the refined parameters, making possible an appropriated discussion. For anatase phase, both compositions, the lattice parameters present the same variation samples and, except for 100°C, the vector a and c values are slightly higher for pure titanium dioxide samples, at least up to 600°C, where the anatase phase for pure titanium dioxide sample becomes unstable (**Figure 3(a)**). By considering tetravalent silicon and zirconium hexacoordinate dopant cations, with ionic radii of 40 pm and 72 pm, respectively, the average radii are close to 56 pm. Therefore, the substituting cations constitute as smaller than hexacoordinate tetravalent titanium substituted one (61 pm). Thus, it is a coherent result that the slight lattice contraction was observed for the Si-Zr doped samples.

Maybe it is not important to explain the basis of the anatase phase stabilization, but the inverse effect that occurred at 100°C is in consequence of the higher amount hydroxyl groups in Si-Zr-doped titanium dioxide dry gel, as was demonstrated in TG analysis. The importance of the Rietveld analysis is established just above the 650°C and remarkable difference is observed among the samples originated from both the compositions. In temperatures close to anatase-to-rutile
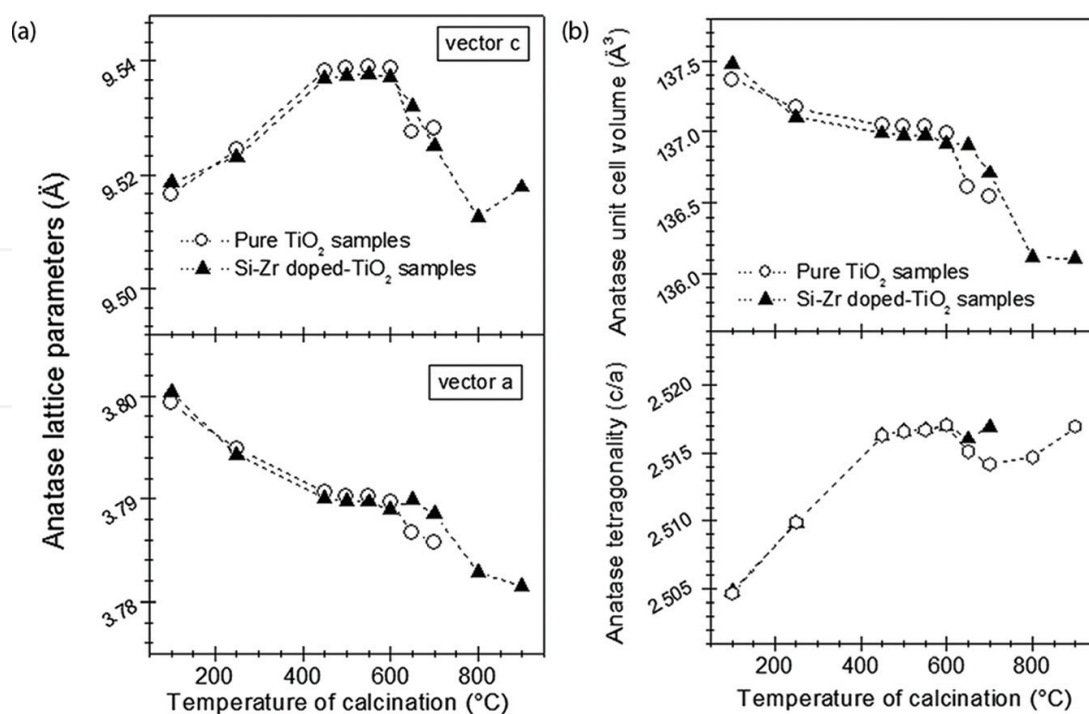
Figure 3. Refined lattice parameters for anatase phase as a function of calcination temperature for: (a) vectors values and (b) calculated unit cell volume and tetragonality (c/a).

phase transition, the both vectors a and c of anatase phase for pure titanium dioxide samples start to reduce, marking the initial collapse of anatase phase, which will no longer be present at 800°C. By observing the same variation for Si-Zr-doped samples, it is possible to observe that behaviour is characteristic of anatase phase crystallization, but only for pure titanium dioxide sample and is followed by the anatase to rutile phase transition.

By observing the variation of anatase cell volume in **Figure 3(b)** it is possible to notice an impressive variation similarity with the variation of vector a (**Figure 3(a)**), for both samples. It is possible to observe the tetragonality changes between the pure and the Si-Zr-doped titanium dioxide samples in the same way, but only displaced to higher temperature for Si-Zr-doped one. Thus, those results corroborate the previous DTA differences and the tetragonality of anatase single phase in the Si-Zr-doped titanium dioxide sample calcined at 900°C is very close to the well-crystallized anatase single phase observed in the pure titanium dioxide sample calcined at 600°C.

The reliable crystallization process was investigated through the size-strain calculation according to the methodology well-established [60] and using tungsten carbide as standard material in order to evaluate the instrumental contributions. It was noticed that the crystallite size stays in low values until the beginning of anatase-to-rutile phase formation and the peak narrowing is originated from the reduction of the lattice microstrain practically (**Figure 4(a)**). Thus, the crystallite coalescence occurs as a consequence of the destroying-rebuilt oxygen-metallic cation bonds process starting at 650°C, regardless of anatase-to rutile phase transition. Beyond that reconstructive transformation, above 700°C, the crystallite sizes considerably increase despite of
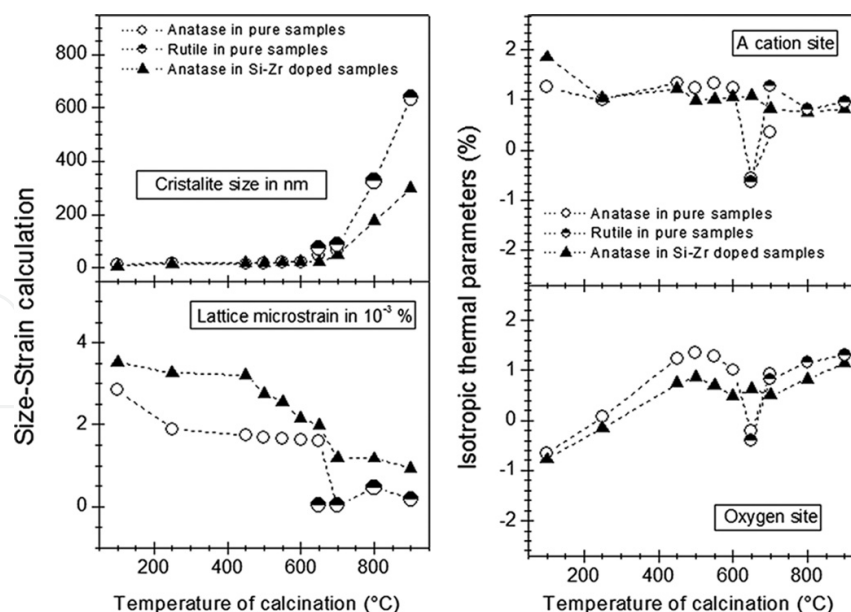
Figure 4. Calculated data through the refined lattice parameters and peak profiles: (a) crystallite size and lattice microstrain and (b) isotropic thermal parameters.

some variation on lattice microstrain. In **Figure 4(b)**, it is possible to observe that the anatase structure starts with spacious oxygen site through the negative values for isotropic thermal parameters. As the atomic scattering is associated to a specific site volume, it is probable that the hydroxyl groups push oxygen atoms away from each other. The isotropic parameters become higher after the dehydroxylation process and that results are coherent with cell volume variation and thermal analysis results. However, for pure titanium dioxide samples, the atoms experience a new localized spacing in the temperature close to the anatase-to-rutile phase transition, different from Si-Zr-doped ones. That event indicates the reconstructive transformation occurs through the destroying-rebuilt bonds, because the variation of the isotropic thermal parameters presents noticeable inflection during that process.

4. Conclusions

The accurate structural characterization was carried out by X-ray diffractometry and rietveld refinement in titanium dioxide sample synthesized through sol-gel method and calcined in wide temperature range in order to evaluate the effects on the thermal stabilization of the zirconium silicate doping at 5 mol%. The discussion of structural variations in both pure and Si-Zr-doped sample compositions was supported by corresponding thermal analysis taken from dry gels and consistent correlations were found.

The silicon and zircon dopants lead to more retention of residues coming from jellying process and also the fresh anatase formed is more hydrolyzed. All of the exothermic events associated to the phase crystallization in both samples are displaced to higher temperatures if compared to the pure titanium dioxide sample. Thus, the final crystallization associated to oxygen vacancies elimination as a function of oxygen incorporation occurs above 900°C.

By observing the X-ray diffraction patterns, it was possible to prove that the Si-Zr dopants at concentration of 5 mol% are able to prevent the rutile phase transition in titanium dioxide samples calcined up to 900°C. But, the rietveld analysis was very important to found the structural basis for that behaviour and the known reconstructive transformation was proved for the anatase-to-rutile phase transition. It was possible to show that the isotropic thermal parameters for oxygen and titanium atoms are considerably affected just during the anatase phase collapse and rutile one rising.

The crystallite coalescence responsible for anatase crystallization does not occur in pure titanium dioxide samples, and the X-ray diffraction peaks narrowing observed for calcined samples in several publications is consequence only of the microstrain reduction. Thus, the pure titanium dioxide samples cannot be crystallized as anatase phase without the parallel rutile phase conversion, different from the Si-Zr-doped titanium dioxide sample. Consequently, well-crystallized anatase single phase at 900°C can be obtained by doping the titanium dioxide samples with 5 mol% of Si-Zr. That composition can become a new semiconductor matrix for the investigation of new dopants in order to improve further the photocatalysis performance or maybe, other possible applications.

Author details

Alberto Adriano Cavalheiro[1]*, Lincoln Carlos Silva de Oliveira[2] and
Silvanice Aparecida Lopes dos Santos[2]

*Address all correspondence to: albecava@gmail.com

1 State University of Mato Grosso do Sul, Naviraí, MS, Brazil

2 Federal University of Mato Grosso do Sul, Campo Grande, MS, Brazil

References

[1] Linsebigler AL, Lu G, Yates JT. Photocatalysis on TiO_2 surfaces: Principles, mechanisms, and selected results. Chemical Reviews. 1995;**95**:735–758. DOI: 10.1021/cr00035a013

[2] Nakata K, Fujishima A. TiO_2 photocatalysis: Design and applications. Journal of Photochemistry and Photobiology C: Photochemistry Reviews. 2012;**13**:169–189. DOI: 10.1016/j.jphotochemrev.2012.06.001

[3] Mills A, Davies RH, Worsley D. Water-purification by semiconductor photocatalysis. Chemical Society Reviews. 1993;**22**:417–425. DOI: 10.1039/CS9932200417

[4] Zhang J, Liu X, Gao S, Huang B, Dai Y, Xu Y, Grabstanowicz LR, Xu T. From AgI/TiO_2 to Ag/TiO_2: Effects of the annealing temperature on the compositions, porous nanostructures,

and visible-light photocatalytic properties. Ceramics International. 2013;**39**:1011–1019. DOI: 10.1016/j.ceramint.2012.07.021

[5] Ibhadon AO, Fitzpatrick P. Heterogeneous photocatalysis: Recent advances and applications. Catalysts. 2013;**3**:189–218. DOI: 10.3390/catal3010189

[6] Sclafani A, Palmisano L, Schiavello M. Influence of the preparation methods of TiO_2 on the photocatalytic degradation of phenol in aqueous dispersion. The Journal of Physical Chemistry. 1990;**94**:829–832. DOI: 10.1021/j100365a058

[7] Cavalheiro AA, Bruno JC, Saeki MJ, Valente JPS, Florentino AO. Effect of scandium on the structural and photocatalytic properties of titanium dioxide thin films. Journal of Materials Science. 2007;**43**(2):602–608. DOI: 10.1007/s10853-007-1743-2

[8] Qiu S, Starr TL. Zirconium doping in titanium oxide photocatalytic films prepared by atomic layer deposition. Journal of the Electrochemical Society. 2007;**154**(6):H472–H475. DOI: 10.1149/1.2718475

[9] Cavalheiro AA, Bruno JC, Valente JPS, Saeki MJ, Florentino AO. Photocatalytic decomposition of diclofenac potassium using silver-modified TiO_2 thin films. Thin Solid Films. 2008;**516**(18):6240–6244. DOI: 10.1016/j.tsf.2007.11.117

[10] Liu S. Liu X, Chen Y, Jiang R. A novel preparation of highly active iron-doped titania photocatalysts with a p-n junction semiconductor structure. Journal of Alloys and Compounds. 2010;**506**(2):877–882. DOI: 10.1016/j.jallcom.2010.07.103

[11] Su D, Dou S, Wang G. Anatase TiO_2: Better anode material than amorphous and rutile phases of TiO_2 for Na-Ion batteries. Chemistry of Materials. 2015;**27**(17):6022–6029. DOI: 10.1021/acs.chemmater.5b02348

[12] Orera VM, Merino RI. Ceramics with photonic and optical applications. Boletín de la Sociedad Española de Cerámica y Vidrio. 2015;**54**(1):1–10. DOI: 10.1016/j.bsecv.2015.02.002

[13] Schneider J, Matsuoka M, Takeuchi M, Zhang J, Horiuchi Y, Anpo M, Bahnemann DW. Understanding TiO_2 photocatalysis: Mechanisms and materials. Chemical Review. 2014;**114**(19):9919–9986. DOI: 10.1021/cr5001892

[14] Pesci FM, Wang G, Klug DR, Li Y, Cowan† AJ. Efficient suppression of Electron–hole recombination in oxygen-deficient hydrogen-treated TiO_2 nanowires for photoelectrochemical water splitting. The Journal of Physical Chemistry C, Nanomaterials and Interfaces. 2013;**117**(48):25837–25844. DOI: 10.1021/jp4099914

[15] Vargas S, Arroyo R, Haro E, Rodriguez R. Effect of cationic dopants on the phase transition temperature of titania prepared by the sol-gel method. Journal of Materials Research. 1999;**14**(10):3932–3937. DOI: 10.1557/JMR.1999.0532

[16] Moezzi A, McDonagh AM, Cortie MB. Zinc oxide particles: Synthesis, properties and applications. Chemical Engineering Journal 2012;**185-186**:1–22. DOI: 10.1016/j.cej.2012.01.076

[17] Gonsález MP, Tomás SA, Luna MM, Arvizu MA, Cruz MMT. Optical, structural, and morphological properties of photocatalytic TiO_2–ZnO thin films synthesized by the sol-gel process. Thin Solid Films. 2015;**594**:304–309. DOI: 10.1016/j.tsf.2015.04.073

[18] Wang S, Pan L, Song J-L, Mi W, Zou J-J, Wang L, Zhang X. Titanium-defected undoped anatase TiO_2 with p-Type conductivity, oom-temperature ferromagnetism, and remarkable photocatalytic performance. Journal of the American Chemical Society. 2015;**137** (8):2975–2983. DOI: 10.1021/ja512047k

[19] Yalçin Y, Kiliç M, Çinar Z. Fe^{+3}-doped TiO_2: A combined experimental and computational approach to the evaluation of visible light activity. Applied Catalysis B: Environmental. 2010;**99**(3-4):469–477. DOI: 10.1016/j.apcatb.2010.05.013

[20] Jamalluddin NA, Abdullah AZ. Reactive dye degradation by combined Fe(III)/TiO_2 catalyst and ultrasonic irradiation: Effect of Fe(III) loading and calcination temperature. Ultrasonics Sonochemistry. 2011;**18**(2):669–678. DOI: 10.1016/j.ultsonch.2010.09.004.

[21] Niu Y, Xing M, Zhang J, Tian B. Visible light activated sulfur and iron co-doped TiO_2 photocatalyst for the photocatalytic degradation of phenol. Catalysis Today. 2013;**201** (1):159–166, DOI: 10.1016/j.cattod.2012.04.035

[22] Harizanov O, Harizanova A. Development and investigation of sol-gel solutions for the formation of TiO_2 coatings. Solar Energy Materials and Solar Cells. 2000;**63**(2):185–195. DOI: 10.1016/S0927-0248(00)00008-8

[23] Katoh R, Furube A, Yamanaka K, Morikawa T. Charge separation and trapping in N-doped TiO_2 photocatalysts: A time-resolved microwave conductivity study. The Journal of Physical Chemistry Letters. 2010;**1**(22):3261–3265. DOI: 10.1021/jz1011548

[24] Batzill M, Morales EH, Diebold U. Influence of nitrogen doping on the defect formation and surface properties of TiO_2 rutile and anatase. Physical Review Letters. 2006;**96** (2):026103. DOI: 10.1103/PhysRevLett.96.026103

[25] Wetchakun N, Incessungvorn B, Wetchakun K, Phanichphant S. Influence of calcination temperature on anatase to rutile phase transformation in TiO_2 nanoparticles synthesized by the modified sol–gel method. Materials Letters. 2012;**82**:195–198. DOI: 10.1016/j. matlet.2012.05.092

[26] Wu S-X, Zhi M, Qin Y-N, He F, Jia L-S, Zhang Y-J. XPS study of Cooper dopping TiO_2 photocatalyst. Acta Physico-Chimica Sinica. 2003;**19**(10):967–969. DOI: 10.3866/PKU. WHXB20031017

[27] Liu X, Dong G, Li S, Lu G, Bi Y. Direct observation of charge separation on anatase TiO_2 crystals with selectively etched {001} facets. Journal of the American Chemical Society. 2016;**138**(9):2917–2920. DOI: 10.1021/jacs.5b12521

[28] Hanaor DAH, Sorrell CC. Review of the anatase to rutile phase transformation. Journal of Materials Science. 2011;**46**(4):855–874. DOI: 10.1007/s10853-010-5113-0

[29] Hanaor DAH, Assadi MHN, Li S, Yu A, Sorrell CC. Ab initio study of phase stability in doped TiO$_2$. Computational Mechanics. 2012;**50**(2):185–194. DOI: 10.1007/s00466-012-0728-4

[30] Selloni A. Crystal growth: Anatase shows its reactive side. Nature Materials. 2008;**7** (8):613–615. DOI: 10.1038/nmat2241

[31] Setvin M, Aschauer U, Hulva J, Simschitz T, Daniel B, Schmid M, Selloni A, Diebold U. Following the reduction of oxygen on TiO$_2$ anatase (101) step by step. Journal of the American Chemical Society. 2016;**138**(30):9565–9571. DOI: 10.1021/jacs.6b04004

[32] Zaleska A. Doped-TiO$_2$: A review. Recent Patents on Engineering. 2008;**2**(3):157–164. DOI:10.2174/187221208786306289

[33] Zhu S-C, Xie S H, Liu Z-P. Nature of rutile nuclei in anatase-to-rutile phase transition. Journal of the American Chemical Society. 2015;**137**(35):11532–11539. DOI: 10.1021/jacs.5b07734

[34] Li B, Wang X, Yan M, Li L. Preparation and characterization of nano-TiO$_2$ powder. Materials Chemistry and Physics. 2003;**78**(1):184–188. DOI: 10.1016/S0254-0584(02)00226-2

[35] Hu Y, Tsai HL, Huang CL. Phase transformation of precipitated TiO$_2$ nanoparticles. Materials Science and Engineering: A. 2003;**344**(1-2):209–214. DOI: 10.1016/S0921-5093 (02)00408-2

[36] Look JL, Zukoski DF. Colloidal stability and titania precipitate morphology: Influence of short-range repulsion. Journal of the American Ceramic Society. 1995;**78**(1):21–32. DOI: 10.1111/j.1151-2916.1995.tb08356.x

[37] Ahn YU, Kim EJ, Kim HT, Hahn SH. Variation of structural and optical properties of sol-gel TiO$_2$ thin films with catalyst concentration and calcination temperature. Materials Letters. 2003;**57**(30):4660–4666. DOI: 10.1016/S0167-577X(03)00380-X

[38] Hemissi M, Adnani HA. Optical and structural properties of titanium oxide thin films prepared by sol-gel methods. Digest Journal of Nanomaterials and Biostructures. 2007;**2** (4):299–305. Available from: www.chalcogen.ro/index.php/journals/digest-journal-of-nanomaterials-and-biostructures. [Accessed: 15-Feburary-2017].

[39] Chaudhary V, Srivastava AK, Kumar J. On the sol-gel synthesis and characterization of titanium oxide nanoparticles. Materials Research Society Symposia Proceedings. 2001;**1352**(11):10–24. DOI: 10.1557/opl.2011.759

[40] Nagpal VJ, Davis RM, Riffle JS. In situ steric stabilization of titanium dioxide particles synthesized by a sol-gel process. Colloids and Surfaces A: Physicochemical and Engineering Aspects. 1994;**87**(1):25–31. DOI: 10.1016/0927-7757(93)02735-W

[41] Saleh A, Rasin FA, Ameen MA. TiO$_2$ nanoparticles prepared by sol-gel. Journal of Materials Science and Engineering. 2009;**3**(12):81–84. Serial No. 25. Available from: www.davidpublishing.com/davidpublishing/upfile/8/5/2012/2012080582702945.pdf. [Accessed: 14-Feburary-2017]

[42] Hayle ST, Gonfa GG. Synthesis and characterization of titanium oxide nanomaterials using sol-gel method. American Journal of Nanoscience and Nanotechnology. 2014;**2**(1):1–7. DOI: 10.11648/j.nano.20140201.11

[43] Nadzirah S, Foo KH, Hashim U. Morphological reaction on the different stabilizers of titanium dioxide nanoparticles. International Journal of Electrochemical Science. 2015;**10**:5498–5512. Available from: www.electrochemsci.org/papers/vol10/100705498.pdf [Accessed: 15 Feburary 2017].

[44] Vorkapic D, Matsoukas T. Effect of temperature and alcohols in the preparation of titania nanoparticles from alkoxides. Journal of the American Ceramic Society. 1998;**81**(11):2815–2820. DOI: 10.1111/j.1151-2916.1998.tb02701.x

[45] Lukáč J, Klementová M, Bezdička P, Bakardjieva S, Šubrt J, Szatmáry L, Bastl Z, Jirkovský J. Influence of Zr as TiO_2 doping ion on photocatalytic degradation of 4-chlorophenol. Applied Catalysis B-Environmental. 2007;**74**(1-2):83–91. DOI: 10.1016/j.apcatb.2007.01.014

[46] Shannon RD. Revised effective ionic radii and systematic studies of interatomic distances in halides and chalcogenides. Acta Crystallographica Section A, Foundations of Crystallographica. 1976;**A32**:751–767. DOI:10.1107/s0567739476001551

[47] Harraz FA, Salam OEA, Mostafa AA, Mohamed RM, Hanafy M. Rapid synthesis of titania-silica nanoparticles photocatalyst by a modified sol-gel method for cyanide degradation and heavy metals removal. Journal of Alloys and Compounds. 2013;**551**:1–7. DOI: 10.1016/j.jallcom.2012.10.004

[48] Okada K, Yamamoto N, Kameshima Y, Yasumori A. Effect of silica additive on the anatse to rutile phase transition. Journal of the American Ceramic Society. 2001;**84**(7):1591–1596. DOI: 10.1111/j.1151-2916.2001.tb00882.x

[49] Reidy DJ, Holmes JD, Morris MA. Preparation of a highly thermally stable titania anatase phase by addition of mixed zirconia and silica dopants. Ceramics International. 2006;**32**(3):235–239. DOI: 10.1016/j.ceramint.2005.02.009

[50] Badli NA, Ali R, Yuliati L. Influence of zirconium doped titanium oxide towards photocatalytic activity of paraquat. Advanced Materials Research. 2015;**1107**:377–382. DOI: 10.4028/www.scientific.net/AMR.1107.377

[51] Kitiyanan A, Ngamsinlapasathian S, Pavasupree S, Yoshikawa S. The preparation and characterization of nanostructured TiO_2-ZrO_2 mixed oxide electrode for efficient dye-sensitized solar cells. Journal of Solid State Chemistry. 2005;**178**(4):1044–1048. DOI: 10.1016/j.jssc.2004.12.043

[52] Ding Z, Hu X, Lu GQ, Yue P-L, Greenfield PF. Novel silica gel supported TiO_2 photocatalyst synthesized by CVD method. Langmuir. 2000;**16**(15):6216–6222. DOI: 10.1021/la000119l

[53] Ilkhechi NN, Kaleji BK. Effect of Cu2+, Si4+ and Zr4+ dopant on structural, optical and photocatalytic properties of titania nanopowders. Optical and Quantum Electronics. 2016;**48**(347):5–9. DOI: 10.1007/s11082-016-0621-z

[54] Joint Committee on Powder Diffraction Standards (JCPDS). International Center for Diffraction Data. Philadelphia; 2003.

[55] Inorganic Crystal Structure Database (ICSD). Version 1.3.1.Eggenstein-Leopoldshafen: FIZ Karlsruhe; 2003

[56] Rietveld HM. A profile refinement method for nuclear and magnetic structures. Journal of Applied Crystallography. 1969;**2**:65–71. DOI: 10.1107/S0021889869006558

[57] Young RA, Sakthive AL, Moss TS, Paiva-Santos CO. DBWS-9411—an upgrade of the DBWS programs for Rietveld Refinement with PC and mainframe computers. Journal of Applied Crystallography. 1995;**28**:366–367. DOI: 10.1107/S0021889895002160

[58] Young RA, Larson AC, Paiva-Santos CO. User's Guide to Program DBWS-9807a for Rietveld Analysis of X-ray and Neutron Powder Diffraction Patterns with a PC and Various Other Computers. Atlanta, GA: School of Physics Georgia Institute of Technology; 2000. DOI: 10.1.1.469.7262

[59] Strunk J, Vining WC, Bell AT. A study of oxygen vacancy formation and annihilation in submonolayer coverages of TiO_2 dispersed on MCM-48. Journal of Physics and Chemistry. 2000;**C**(114):16937–16945. DOI: 10.1021/jp100104d

[60] Paiva-Santos CO, Cavalheiro AA, Zaghete MA, Cilense M, Varela JA, Giotto MTS, Mascarenhas YP. An XRD study of the structure and microstructure of the laboratory synthesized crystals of $MgNb_2O_6$(NM) and PbMg1/3Nb2/3O3 (PMN). Advances in X-Ray Analysis. 2001;**44**:38–43. DOI: 10.1.1.296.1602